Synthesis, characterization and biomedical applications of Berberine–Cuo nanoparticles for non-small cell lung cancer therapy

Sakthivel Manju Bargavi[1], Malchi Suresh[2], Narayanan Doss Prabhavathy Devi[1]* and Kodaganti Naresh Kumar[2]
1. Department of Nutrition and Dietetics, Faculty of Humanities and Science, Meenakshi Academy of Higher Education and Research, K.K. Nagar, Chennai-600 078, INDIA
2. Department of Research, Meenakshi Academy of Higher Education and Research, K.K. Nagar, Chennai-600 078, INDIA
*prabhavathy_devi@yahoo.com

Abstract

Lung cancer remains a leading cause of cancer-related mortality worldwide, especially NSCLC is the majority of cases affecting patients' survival and quality of life. Conventional treatments are often limited by high cost, dose-limiting toxicity and poor therapeutic outcomes. To address these challenges, we developed an eco-friendly synthesis of berberine-incorporated copper oxide nanoparticles (BER-CuONPs) using Solanum torvum *(Turkey berry). The synthesis was confirmed by a characteristic color change (yellow to olive green) and UV–visible spectroscopy with a maximum absorption peak at 400–450 nm. Characterization by SEM-EDX, TEM, Zeta potential and AFM revealed spherical, well-dispersed nanoparticles with an average size of ~22 nm, moderate stability, controlled surface roughness and favorable physicochemical properties for biomedical applications.*

The cytotoxicity effect of BER-CuONPs demonstrated enhanced anticancer activity with a significantly lower IC50 value (49.9 ± 2 µg/mL) compared to BER (122.4 ± 2 µg/mL) and CuONPs (147 ± 2 µg/mL) in NCI-H460 cells, while retaining low toxicity in HEK-293 cells. The wound healing assay confirmed dose-dependent inhibition of cell migration and AO/EtBr staining validated apoptosis induction comparable to cisplatin. Therefore, BER-CuONPs represent a promising multifunctional nanoplatform for NCI-H460 cells. Future studies should focus on in vivo validation, mechanistic pathways, pharmacokinetics and systemic toxicity for clinical translation.

Keywords: Apoptosis, Anti-cancer activity, Berberine, Copper oxide nanoparticles, NCI-H460 cells.

Introduction

According to estimates, there were emerging cancer cases of 19.3 million worldwide in 2020 by the Global Cancer Observatory. India secured the third position followed by China and the United States, for the incidence of cancer. GLOBOCAN further predicts that the number of new cases of cancer occurrence will rise by 57.5% from 2020, reaching 2.08 million by 2040 [22] Among them, the most predominant cancer-related death is lung cancer, contributing to the maximum death rates among males and females. The major common reason is smoking, which accounts for approximately 85% of total lung cancer occurrences. Usually, the diagnosis of lung cancer is identified at advanced stages; therefore, the treatment facilities are also limited[9].

Nowadays, traditional cancer treatments are limited to surgery, radiation and chemotherapy, which can affect the normal tissues or may partially eliminate cancer cells. At present, platinum-based drugs are used in NSCLC chemotherapy treatments particularly cisplatin is frequently used due to its cost effectiveness and strong anti-tumor effect; however, 50% NSCLC patients show cisplatin resistance due to intrinsic changes and influences of tumor microenvironment such as enhanced DNA repair mechanism, reduced cellular uptake, inhibition of apoptosis, drug efflux and also caused nephrotoxicity in normal cells[7].

Therefore, a better alternative source for cancer therapy is nanotechnology which selectively targets the cancer cells and neoplasms, optimizes surgical tumor removal and enhances the efficacy of chemotherapy. In the present study, the application of nanomedicine in nanotechnology has transformed and extended both the diagnosis of cancer and facilitated the development of nanotechnology-assisted chemotherapy, with the potential to significantly improve cancer therapy[17.] The main advantage of using nanotechnology-based cancer treatment is to enhance drug delivery, improve therapeutic efficacy, reduce side effects, selectively target tumors via mechanisms and even at high dosages of anticancer drugs at the tumor site with minimal exposure to healthy cells and promising for NSCLC treatment[13].

Solanum torvum (Turkey berry) is a traditional medicinal, tiny shrub that is associated with the *Solanaceae* Juss and grows widely in tropical regions throughout Thailand and is known as "Turkey Berry" and contains approximately 3000 species. The availability and affordability of *S. torvum* make it a more sustainable choice for large-scale applications like green nanoparticle synthesis[6].

Copper nanoparticles are inorganic due to being easily oxidized to form copper oxides (CuO). The copper has its potential for broad-spectrum bioactivity with cost-effectiveness compared to noble metals and is easy to synthesize. Therefore, both copper and its nanoparticles

have been broadly applied as diagnostic tools and targeted drug delivery for various diseases, particularly in anti-cancer, radiotherapy and radiation dosimetry and their ability to associate with the cellular level, providing multifunctional reactions in our human body [12].

Berberine is an isoquinoline alkaloid chemically known as (2,3-methylenedioxy-9,10-dimethoxyprotoberberine chloride) quinolizinium present in many parts of plants such as stems, rhizomes, roots, the outer layer of the trunk, flowers and acrid fruits of *Coptis chinensis* including various *Berberidaceae* species[5]. It can also be used for the treatment of many diseases like cancer, cardiovascular, neurological disorders, diabetes, lipid balance, nonalcoholic fatty liver disease and particularly against digestive diseases. Research has found that berberine is a potent anticancer and chemosensitizer that prevents the replication of cells in many cancer cells and disrupts the interaction with tissue infiltration and cancer cell dissemination[21].

Berberine has exhibited many biological benefits but it has its limitations such as poor bioavailability when administered orally than intravenously due to first-pass effects in the intestinal lumen, leading to drawbacks in clinical application. To overcome these challenges, berberine can be formulated via an eco-friendly approach to improve therapeutic potential in NSCLC[4]. Therefore, recently, studies have evidenced that berberine can be used for targeted drug delivery via nanotechnology-based approaches[1].

The present study primarily aims to synthesize and optimize berberine conjugated copper oxide nanoparticles (BER-CuONPs) using the green synthesis approach mediated by *S. torvum* (Turkey berry) and to investigate their therapeutic potential against non-small cell lung cancer (NCI-H460). The objective of the present study is to prepare and characterize BER-CuONPs using eco-friendly plant-mediated synthesis and to evaluate the anti-cancer and anti-migration effect of BER-CuONPs using MTT assay and wound healing assay, along with apoptotic assay in NSCLC. Cisplatin is the chemotherapeutic drug used for the positive control.

Material and Methods

Green synthesis of berberine-loaded copper oxide nanoparticles: Fresh *Solanum torvum* (Turkey berry) was purchased in Chennai and authenticated at the Siddha Central Research Institute, Chennai. The plant material was washed thoroughly with distilled water, dried completely and finely ground using a manual grinder. One gram of the powdered sample was mixed with 100 mL of distilled water, boiled at 70 °C for 30 minutes and the supernatant was collected. 30 mL of the extract was added to 70 mL of 20 mM $CuSO_4$ solution and maintained at a neutral pH. The mixture was stirred at 750 rpm for 24 hours to obtain *S. torvum* mediated copper oxide nanoparticles (CuONPs).

For the preparation of the berberine nanoformulation, 100 mg of berberine chloride (BBR-Cl) was dissolved in 1 mL of dimethyl sulfoxide (DMSO) and 4 mL of phosphate-buffered saline (PBS) and stirred at 750 rpm for 1 hour. Berberine-loaded CuONPs (BER-CuONPs) were synthesized by mixing the berberine chloride solution and *S. torvum* (Turkey berry)-mediated CuONP solution in a 1:1 ratio, followed by sonication for 1 hour. The mixture was then dried in a hot-air oven at 60 °C for 5 hours and the air-dried powder was collected for further characterization and biological applications, as shown in figure 1.

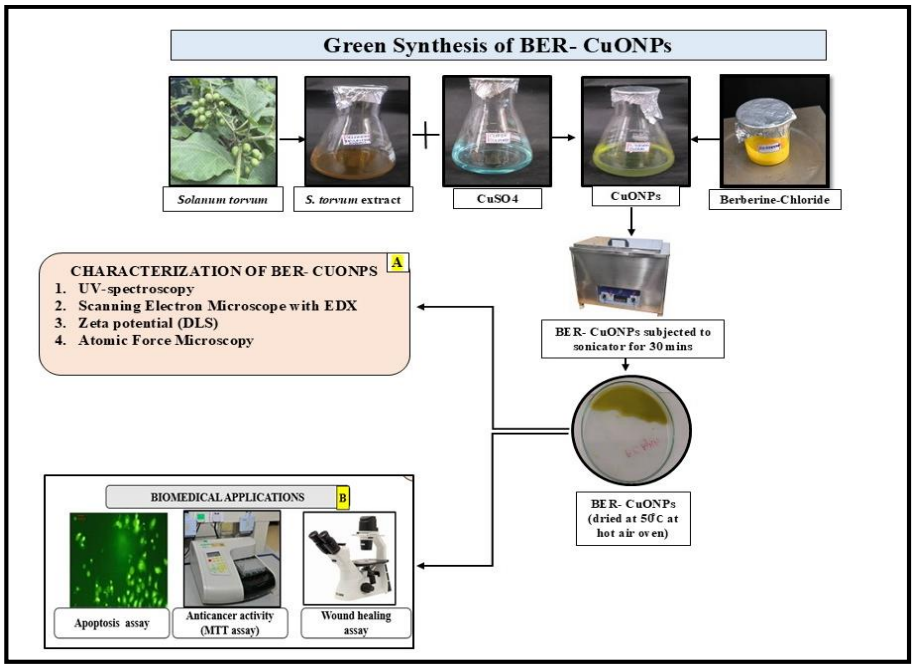

Figure 1: The preparation of berberine-conjugated copper oxide nanoparticles mediated by *Solanum torvum* (Turkey berry)

Characterization of BER-CuONPs: The synthesized BER-CuONPs were confirmed through various characterization techniques, including UV-visible spectroscopy (Shimadzu UV-1900), performed within a wavelength range of 200-700 nm. Surface morphology and elemental composition were assessed using Scanning Electron Microscopy (SEM) and Energy Dispersive X-ray (EDX) analysis (Carl Zeiss model sigma 300). A Transmission Electron Microscope was used to determine the size, shape and structure of the nanoparticles (HR-TEM) (Talos F200S High-Resolution Scanning TEM). Additionally, Atomic Force Microscopy (AFM) was used to investigate the three-dimensional structure of the green-synthesized copper oxide nanoparticles. Dynamic Light Scattering (DLS) was used to determine the hydrodynamic size distribution and surface charge (zeta potential) of the nanoparticles.

Cell culture: NCI-H460 Non-Small Cell Lung Cancer (NCI-H460) cell lines and Human Embryonic Kidney cells (HEK-293) were procured from the National Centre for Cell Science (NCCS), Pune, India. Cells were cultured in Dulbecco's Modified Eagle's medium (DMEM) supplemented with 10% heat-inactivated fetal bovine serum (FBS) and 5% penicillin–streptomycin (10,000 U/mL). Cultures were maintained at 37 °C in a humidified atmosphere containing 5% CO_2 until reaching approximately 90% confluence.

Cell Viability Assay: The cytotoxic effects of CuONPs, BER, BER-CuONPs and cisplatin were evaluated against NCI-H460 cells and HEK-293 using the MTT assay. Briefly, 5×10^3 cells were seeded into 96-well plates and incubated for 24 h to allow cell attachment. The cells were then treated with varying concentrations of 0, 25, 50, 75 and 100 µg/mL of the respective compounds and incubated for an additional 24 h in a CO_2 incubator. Following treatment, the medium was removed and replaced with 110 µL of fresh medium containing SDS-HCl solution. Plates were incubated for 4–18 h to solubilize the formazan crystals. Absorbance was measured at 570 nm using a microplate ELISA reader. All experiments were conducted in triplicate and the percentage of cell viability was calculated by Hanif et al[11].

Wound healing analysis: The cell migration of NCI-H460 cells was assessed using a wound healing assay. Briefly, 5×10^6 cells were seeded into 6-well plates containing complete growth medium and incubated for 24 h to allow monolayer formation. A uniform scratch was created across the cell monolayer using a 200 µL micropipette tip and the wells were gently rinsed with PBS to remove detached cells and debris. The cells were then treated with varying concentrations of BER-CuONPs at 0, 25, 50, 75 and 100 µg/mL and cisplatin, incubated for 24 h. Cell migration into the wound area was monitored using an inverted microscope and images were captured at 0 h and 24 h. The percentage of wound closure was quantified and all experiments were performed in triplicate[27].

AO/EtBr Fluorescence Microscopy Analysis: AO/EB staining was performed with slight modifications to the method described by Mohamed et al[14]. NCI-H460 cells were seeded at a density of 5×10^5 cells per well in a 12-well plate and incubated overnight to allow cell attachment. The cells were then treated with varying concentrations of BER–CuONPs and a high concentration of cisplatin for 24 h. Following treatment, the cells were washed twice with phosphate-buffered saline (PBS) to remove residual medium and unattached cells. Subsequently, they were stained with a freshly prepared mixture of acridine orange and ethidium bromide (1:1, 10 µM) for 15 min at room temperature in the dark. Stained cells were immediately examined under a confocal laser scanning microscope to distinguish viable, apoptotic and necrotic populations based on differential fluorescence emission.

Statistical analysis: Statistical analyses were performed using Microsoft Excel and IBM SPSS Statistics v19 (IBM, Chicago, USA). Data (n = 3) are presented as Mean ± SD. The Shapiro–Wilk test was used to verify normality, followed by parametric analysis. Intra-group comparisons were conducted using paired t-tests, while inter-group differences were assessed by one-way ANOVA. The statistical significance was considered $p < 0.05$.

Results and Discussion

Visual and Spectroscopic characterization of BER-CuONPs: The aqueous extract of *Solanum torvum* (Turkey berry) exhibited a golden-yellow color, which, upon mixing with copper sulfate solution (blue), resulted in a visible color change to olive-green, initially confirming the formation of copper oxide nanoparticles (CuONPs). Similar research has shown that the colour changes resulting from the extraction of copper oxide nanoparticles, such as those found in *Psidium guajava leaf*, *Solanum tuberosum* and *Moringa oleifera*[10,19,25]. This green synthesis approach offers distinct advantages, as it is eco-friendly by eliminating the need for toxic chemicals, is cost-effective due to the use of readily available plant extracts and scalable for large-scale production.

Moreover, the phytochemicals present in *S. torvum* act as natural reducing, capping and stabilizing agents, thereby controlling particle size, preventing agglomeration and improving nanoparticle stability. Importantly, the biocompatible nature and reduced toxicity of these green-synthesized CuONPs make them highly suitable for biomedical applications, particularly in anticancer research. The dual benefits of enhanced stability and sustainable production further highlight the therapeutic potential of *S. torvum*-mediated CuONPs in cancer therapy[10,25].

UV-Visible spectroscopy of BER-CuONPs: The UV–Visible absorption spectra of CuONPs and BER–CuONPs revealed distinct optical properties indicating successful functionalization of nanoparticles with berberine. The CuONPs (black curve) showed a broad absorption peak in

the range of 250–380 nm, characteristic of CuO nanoparticles due to their intrinsic band gap transitions. In contrast, BER–CuONPs (red curve) exhibited a noticeable shift with a strong and broad absorption extending from 250 nm to nearly 600 nm, with a prominent peak around ~460 nm, which can be attributed to the surface plasmon resonance (SPR) effect modified by the conjugation of berberine molecules (Figure 2). This red-shift and enhanced absorption intensity suggests effective surface interaction and capping of CuONPs by berberine, leading to altered electronic transitions and improved stability of the nanocomposite. Previous findings recorded similar peak absorbance of copper oxide nanoparticles of VeA-CuONPs of 412nm[3].

Scanning Electron Microscope with EDX: The SEM micrograph revealed that the synthesized BER–CuONPs exhibited a predominantly rod-like and irregular crystalline morphology, with a tendency to form agglomerated clusters. The average particle size was estimated to be approximately 107 nm, confirming their nanometric nature and the successful formation of nanoparticles (Figure 3). Previous studies also confirmed that the green synthesis of CuO-NPs using Aloe vera extract and *Ralstonia solanacearum* showed similar morphology and particle sizes[20,24,26].

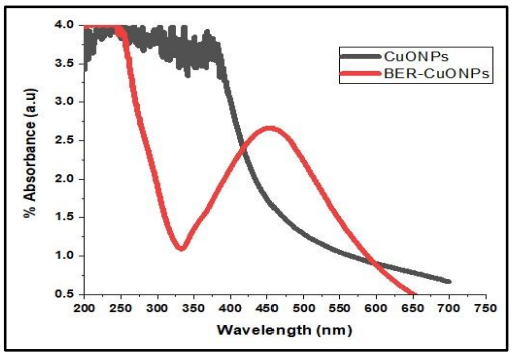

Figure 2: The pictorial image represents the UV-visible spectroscopy of CuONPs and BER-CuONPs

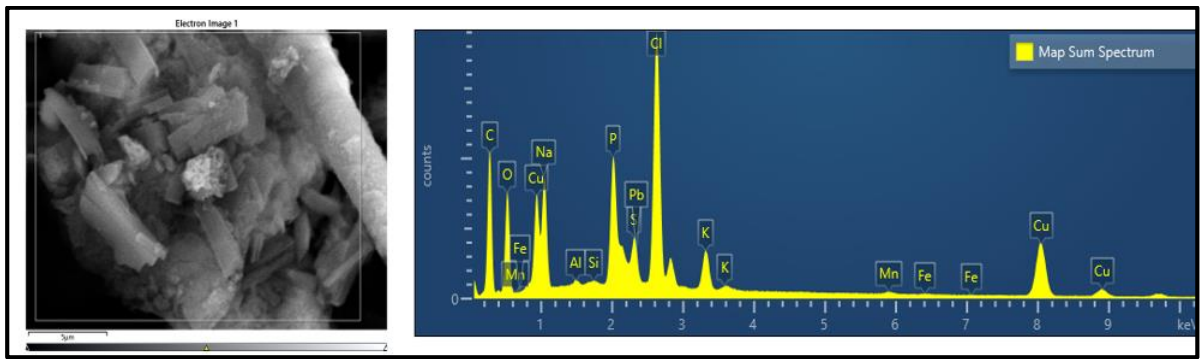

Figure 3: The diagram illustrates the Scanning Electron Microscope with Energy Dispersive X-ray of BER-CuONPs

Table 1
Elemental composition of BER-CuONPs

Element	Weight %	Weight % Sigma	Atomic %
C- Carbon	55.17	0.31	72.37
O- Oxygen	16.28	0.15	16.03
Na- Sodium	4.33	0.05	2.96
Al- Aluminium	0.13	0.01	0.08
Si- Silicon	0.06	0.01	0.03
P- Phosphorus	2.76	0.03	1.41
S- Sulfur	0.94	0.02	0.46
Cl- Chlorine	7.26	0.06	3.23
K- Potassium	1.41	0.02	0.57
Mn- Manganese	0.18	0.02	0.05
Fe- Iron	0.07	0.02	0.02
Cu- Copper	11.21	0.1	2.78
Pb- Lead	0.2	0.08	0.02
Total	100		100

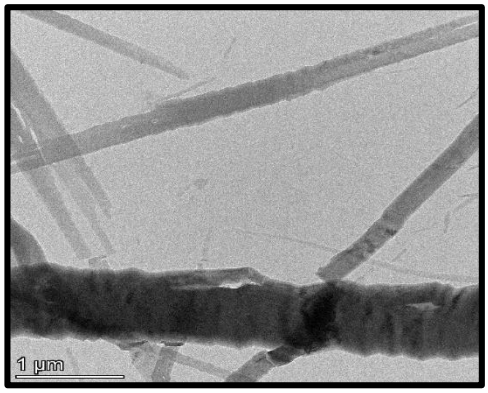

Figure 4: The picture demonstrates the Transmission Electron Microscope of BER-CuONPs

SEM coupled with Energy Dispersive X-ray Spectroscopy (EDS) confirmed the elemental composition of BER–CuONPs, showing C, O and Cu as major constituents along with trace elements. Analysis further showed a high carbon content (55.17 wt%), supporting the berberine conjugation, while oxygen (16.28 wt%) and copper (11.21 wt%) were the major inorganic components, confirming the formation of copper oxide. Chlorine (7.26 wt%) indicated residual precursor salts and trace elements (Na, P, S, K, Mn, Fe, Al, Si, Pb) were also detected, likely from the synthesized compounds as shown in table 1[18].

Transmission Electron Microscope: TEM analysis of BER–CuONPs revealed predominantly rod-like and wire-shaped structures with some smaller irregular particles. The size ranged from 5 to 105 nm, with an average of 22 nm, confirming their nanoscale nature. Some aggregation was observed, likely due to high surface energy, which may support sustained drug release. The rod-like morphology provides a larger surface area and may enhance cellular uptake, suggesting favorable properties for biomedical applications (Figure 4). Similar findings also suggested that the green synthesis of CuO nanorods using *Muntingia calabura* leaves demonstrated a similar particle size of 61.48nm and rod-shaped nanoparticles[20], while *Momordica charantia* showed 79-90nm[18].

Dispersive Light Scattering: DLS is known as quasi-light scattering. Zeta potential is applied for assessing both the surface charge and particle size distribution. During electrophoresis, the surface charge determines the electrode to which particles move. The DLS assessment revealed a well-distributed particle system with a dominant peak at 0.6829 nm, suggesting the presence of smaller, well-dispersed nanoparticles. The moderate polydispersity index (PDI: 0.3447) reflects a reasonably stable formulation with a controlled size distribution, making it suitable for biological interactions. Additionally, the Z-average size of 9018 nm suggests the possible formation of nanoparticle aggregates, which may enhance the sustained release of berberine, leading to prolonged therapeutic effects. Similar findings showed that the extract of the *Catharanthus Roseus* plant Leaf in copper oxide nanoparticles was found to be – 1.88 mV[8]. The zeta potential measurement further supports the formulation stability, with a mean surface charge of 0.4715 mV. Although the value is relatively low, it suggests that the formulation has good compatibility with biological systems, reducing the likelihood of excessive repulsion that could hinder cellular uptake. The moderate zeta deviation (14.38 mV) indicates a balanced charge distribution across the nanoparticles, ensuring effective bioavailability. The berberine copper oxide nanoformulation of synthesized ζ-potential is shown in figure 5.

Atomic Force Microscopy: AFM was demonstrated to examine the characterization of BER-CuONPs in three-dimensional form with sub-nanometer resolution, as depicted in figure 6. The AFM analysis of the copper nanoparticles (CuNPs) conjugated with berberine nanoformulation: The mean surface roughness (Sa: 73.155 nm) and root mean square roughness (Sq: 111.26 nm) indicate a moderately rough surface, suggesting a well-dispersed nanoformulation. The maximum height difference (Sy: 870.4 nm) highlights some degree of nanoparticle aggregation, which could be optimized with stabilizers to enhance uniformity. The peak height (Sp: 597.38 nm) exceeding the valley depth (Sv: -273.02 nm) signifies an overall protruding topography which may enhance biological interactions, such as cellular uptake and adhesion.

Further, the line roughness parameters (Ra: 51.263 nm, Rq: 64.185 nm, Ry: 251.58 nm) suggest a relatively smooth nanoformulation with controlled surface variations, which could aid in the sustained release of berberine. The deflection force values (Mean: 27.8 nN, Line Fit: 18.5 nN) indicate strong adhesion forces, ensuring the mechanical stability of the nanoparticles and optimizing them for biomedical applications including antimicrobial and anticancer therapies. The presence of some aggregation, as indicated by the high Sy value, suggests that further optimization using polymer coatings or surfactants might improve dispersion and enhance its pharmacological efficacy.

Anti-cancer activity of BER-CuONPs on H460 cells and HEK-293 cells: The cytotoxic potential of synthesised CuONPs, BER, BER-CuONPs and the reference chemotherapeutic drug cisplatin was evaluated in H460 and

HEK-293 cell lines using the MTT assay. The cell inhibition percentage was noted at different concentrations of 0, 25, 50, 75 and 100 µg/mL. The results show that all the drug dose-dependent cytotoxic effect was observed in the NCI-H460 cell lines. In H460 cells, CuONPs exhibited a cytotoxic effect (27% at 25 µg/mL - 77% at 100 µg/mL) while BER showed effect (32% at 25 µg/mL - 80% at 100 µg/mL).

However, the combination of BER-CuONPs produced greater inhibition (48% at 25 µg/mL - 92% at 100 µg/mL) and cisplatin, a standard chemotherapeutic drug, showed inhibition (37% at 25 µg/mL- 82% at 100 µg/mL) respectively.

In contrast, HEK-293 normal cells exhibited significantly lower inhibition with all test compounds. CuONPs and BER exhibited moderate inhibition (9% at 25 µg/mL – 31 % at 100 µg/mL) and (8% at 25 µg/mL - 33% at 100 µg/mL) respectively. BER-CuONPs also showed minimal cytotoxicity (5% at 25 µg/mL - 16% at 100 µg/mL). However, cisplatin showed higher cytotoxicity in HEK-293 cells (10% at 25 µg/mL - 47% at 100 µg/mL) shown in figure 7. The IC_{50} values for BER-CuONPs, CuONPs, BER and cisplatin are provided in table 2.

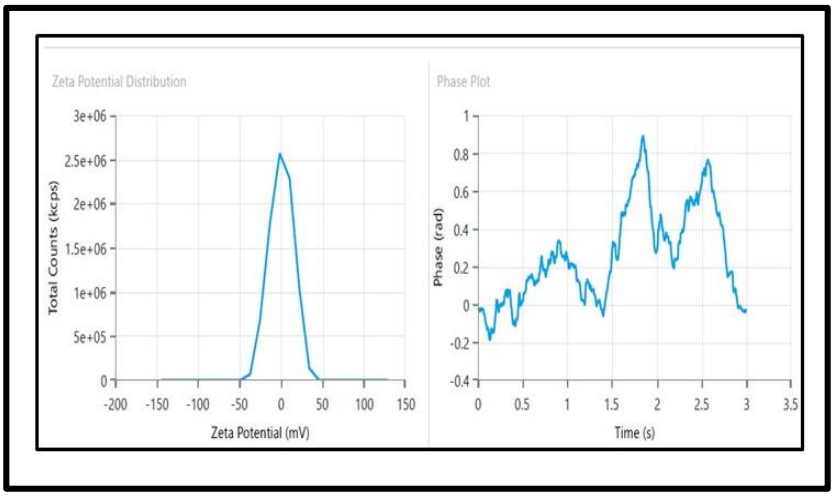

Figure 5: The graphical image depicts the zeta potential of BER-CuONPs

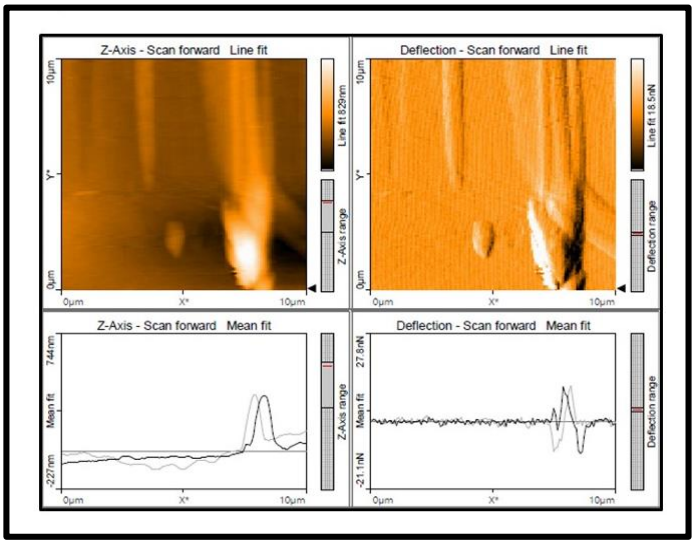

Figure 6: The diagram illustrates the Atomic Force Microscopy (AFM) of BER-CuONPs

Table 2
IC_{50} value by Mean ± SD of CuONPs, BER, BER-CuONPs and Cisplatin

IC_{50} value by Mean ± SD values			
NCI-H460 cells		**HEK-293 cells**	
CuONPs	147.0±2	CuONPs	>100
BER	122.4±2	BER	>100
BER-CuONPs	49.9±1	BER-CuONPs	>100
Cisplatin	84.1±1	Cisplatin	88.3±2

Overall, our results demonstrated that BER-CuONPs showed significantly greater anticancer activity against H460 cells compared to CuONPs, BER and cisplatin. Notably, BER-CuONPs showed lower cytotoxicity towards normal cells (HEK-293), while cisplatin induced greater toxicity. These findings were statistically significant with p-values < 0.05, indicating that BER-CuONPs may offer a more effective and safer alternative for lung cancer treatment. Previously, research has demonstrated the anticancer activity of berberine encapsulated in Poly (lactic-co-glycolic) acid compared with free berberine in MCF-7 cells. The IC_{50} values for berberine nanoparticles were identified as 42 µg/ml, lower than that of berberine at 80 µg/ml, strongly showing its cytotoxicity effects[23].

Similarly, another study has shown the cytotoxic effect of free AuNPs, BBR and a nanoformulation of berberine-loaded gold nanoparticles on liposomes. The cell viability of free AuNPs resulted in 94% at 60µg/mL, exhibiting negligible toxicity in A549 cells. In contrast, BBR revealed a dose-dependent cytotoxic effect of 98% (< 16 µM/mL) and 19% (200 µM/mL) respectively. The nanoformulation (Lipo@AuNPs@BBR) demonstrated significantly better cytotoxicity with an IC_{50} of 80 ±2 µg/ml in single treatment, further reduced to 60 ±4 µg/ml in combination treatment, indicating its superior anticancer activity compared to free forms of AuNPs and BBR [15].

Anti-Migratory Effects of BER-CuONPs on H460 cells: The anti-migratory potential of BER-CuONPs against H460 non-small cell lung cancer (NSCLC) cells were assessed using a scratch wound-healing assay, with cisplatin (100 µg/mL) as a positive control. Cells were treated with BER-CuONPs at 0, 25, 50, 75 and 100 µg/mL for 24 h. Untreated control cells displayed extensive wound closure, indicating high migratory activity. In contrast, BER-CuONPs treatment significantly reduced migration in a dose-dependent manner with wound closure decreasing from 22.00% at 25 µg/mL to 10.19% at 100 µg/mL. Cisplatin-treated cells exhibited 13.87% wound closure in the highest concentrations as illustrated in figure 8. These results demonstrate that BER-CuONPs effectively suppress the migration of NSCLC cells, with statistically significant inhibition ($p < 0.001$), as illustrated in table 3.

Anti-migratory effect of BP-LCN treated at various concentrations like 1, 2.5 and 5µM, in A549 cells observed that the control group showed 49.4± 5.5% wound closure compared with 43.2 ± 3.1, 37.6±0.6 % and 26.3% at 1, 2.5 and 5µM respectively. Therefore, at the highest concentration, there was a drastic reduction in the wound closure than the control group [2].

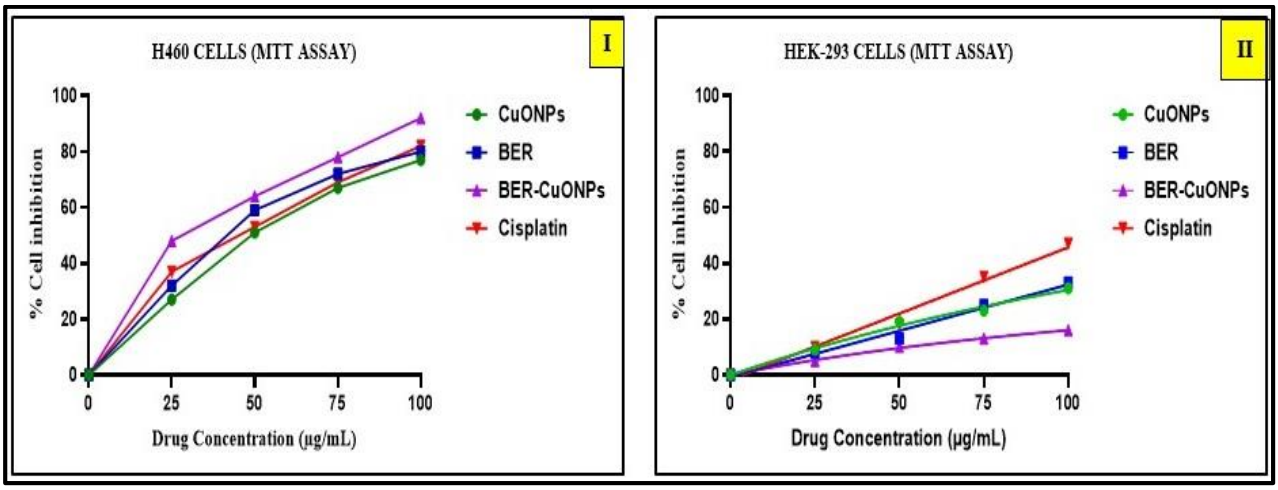

Figure 7: The bar diagram shows the anticancer activity of BER-CuONPs, BER and CuONPs treated at different dosages like 0,25, 50, 75 and 100µg/ml. I) The graphical image illustrated the cytotoxicity of NCI-H460 cells. II) It depicted the effect of anticancer activity in HEK-293 cells

Table 3
Intergroup and intra-group comparisons of migration distance of BER-CuONPs

Drug concentration	0 hours (T_1)	24 hours (T_2)
Control	51.68+1.05	38.26+0.70
25µg/mL	52.32+1.97	42.50+1.37
50µg/mL	50.69+1.21	47.33+1.10
75µg/mL	53.04+1.48	46.03+1.05
100µg/mL	51.93+2.07	48.96+1.52
p-value	**<0.001***	**<0.001***
Paired t-test (intragroup comparisons); 0 hours' vs 24 hours; One Way ANOVA (inter-group comparisons); *p-value<.0.05-statistically significant		

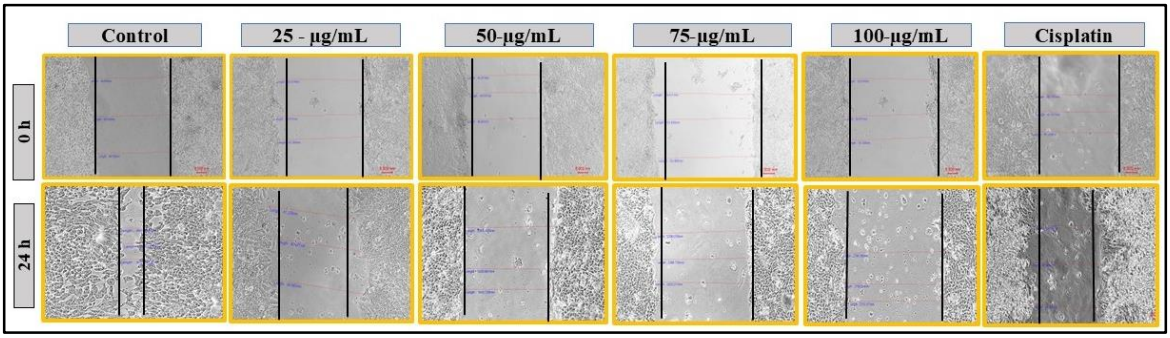

Figure 8: The diagram shows the wound healing response of BER-CuONPs in H460 cells

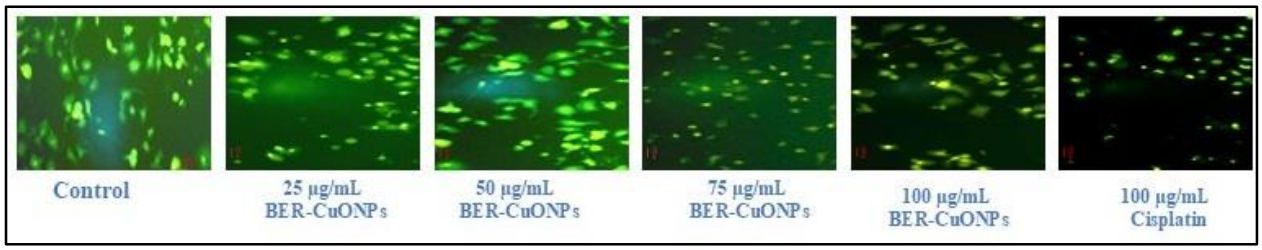

Figure 9: The diagram illustrates the AO/EtBr dual staining of BER-CuONPs in the Apoptosis assay

Apoptotic Assay: AO/EtBr dual staining of H460 cells treated with increasing concentrations of BER–CuONPs demonstrated a dose-dependent induction of apoptosis as evidenced by a progressive shift from green fluorescent viable cells to yellow/orange early apoptotic cells and red late apoptotic/necrotic cells. Untreated control cells exhibited predominantly green fluorescence, indicating high viability with minimal cell death, whereas treatment with 25 and 50 µg/mL BER–CuONPs resulted in a moderate reduction in viable cells and the appearance of early apoptotic populations.

Higher concentrations (75 and 100 µg/mL) markedly decreased green fluorescence with a predominance of orange/red cells indicative of advanced apoptotic and necrotic stages. At 100 µg/mL, BER–CuONPs produced a slightly higher proportion of late apoptotic/necrotic cells compared to 100 µg/mL cisplatin, suggesting marginally greater cytotoxic efficacy as shown in figure 9. These findings confirm that BER–CuONPs possess potent, concentration-dependent anticancer activity against H460 cells, with efficacy at high doses comparable to or exceeding that of cisplatin.

Conclusion

The berberine-conjugated copper oxide nanoparticles were successfully synthesized and characterized, confirming their stability, morphology and conjugation. They demonstrate a strong cytotoxicity effect by reducing cell viability and inhibiting migration in NCI-H460 cells. In normal (HEK-293) cells, the cell viability was 99% indicating no toxicity. In the wound healing assay, it was shown that the changes in wound space at 24h were associated with sustained control release of the drug for a longer duration.

The apoptotic assay showed a potent, dose-dependent cytotoxic efficacy at higher concentrations than cisplatin. These combined properties highlight its multifunctional therapeutic agent for strong anti-cancer cytotoxic potential and reduced cell migration (antimetastatic). While these findings are promising, the study is limited to *in vitro* studies. Future *in vivo* studies, mechanistic evaluations and optimization for targeted delivery are required to confirm their therapeutic efficiency and clinical applicability.

Acknowledgement

The authors express their sincere gratitude to the Department of Central Research Laboratory at Meenakshi Academy of Higher Education and Research, Chennai, for their valuable support and for providing the time and resources necessary to carry out this work.

References

1. Ai X. et al, Berberine: A review of its pharmacokinetics properties and therapeutic potentials in diverse vascular diseases, *Front. Pharmacol.*, **12**, 762654 **(2021)**

2. Alnuqaydan A.M. et al, Evaluation of the cytotoxic activity and anti-migratory effect of berberine–phytantriol liquid crystalline nanoparticle formulation on non-small-cell lung cancer *in vitro*, *Pharmaceutics*, **14(6)**, 1119 **(2022)**

3. Ananda Murthy H.C. et al, Enhanced multifunctionality of CuO nanoparticles synthesized using aqueous leaf extract of *Vernonia amygdalina* plant, *Results Chem.*, **3**, 100141 **(2021)**

4. Becit-Kızılkaya M., Öncü Ş., Şen S. and Çelik S., Berberine synergizes with cisplatin via inducing apoptosis on A549 non-small cell lung cancer cells, *Eur. J. Ther.*, **29**, 1703 **(2023)**

5. Chaudhary P. and Patel H.U., RP-HPLC and spectrophotometric determination of rutin trihydrate, berberine chloride and trigonelline hydrochloride in antidiabetic polyherbal formulations, *Res. J. Pharm. Technol.*, **13(7)**, 3293–3299 **(2020)**

6. Darkwah W.K., Koomson D.A., Miwornunyuie N., Nkoom M. and Puplampu J.B., Phytochemistry and medicinal properties of *Solanum torvum* fruits, *All Life*, **13(1)**, 498–506 **(2020)**

7. Dasari S. and Bernard Tchounwou P., Cisplatin in cancer therapy: molecular mechanisms of action, *Eur. J. Pharmacol.*, **740**, 364–378 **(2014)**

8. Dayana K.S., Jothimani R. and Durai S.C.V., Green synthesis of copper oxide nanoparticles from *Catharanthus roseus* plant leaf extract and its investigation, *J. Nano Electron. Phys.*, **13(1)**, 01014 **(2021)**

9. Dela Cruz C.S., Tanoue L.T. and Matthay R.A., Lung cancer: epidemiology, etiology and prevention, *Clin. Chest Med.*, **32(4)**, 605–644 **(2011)**

10. El-Tanbouly R. et al, Moringa (*Moringa oleifera*) green-synthesized copper oxide nanoparticles for the drought tolerance of tomato (*Solanum lycopersicum*), *BMC Plant Biol.*, **25(1)**, 1–15 **(2025)**

11. Hanif A. et al, Cytotoxicity against A549 human lung cancer cell line via the mitochondrial membrane potential and nuclear condensation effects of *Nepeta paulsenii* Briq., *Molecules*, **28(6)**, 2812 **(2023)**

12. Hussain Z. et al, Nano-scaled materials may induce severe neurotoxicity upon chronic exposure to brain tissues: a critical appraisal and recent updates, *J. Control. Release*, **327**, 733–753 **(2020)**

13. Javed Iqbal M. et al, Nanotechnology-based strategies for berberine delivery system in cancer treatment: pulling strings to keep berberine in power, *Front. Mol. Biosci.*, **8**, 624494 **(2021)**

14. Mohamed Subarkhan M., Prabhu R.N., Raj Kumar R. and Ramesh R., Antiproliferative activity of cationic and neutral thiosemicarbazone copper (II) complexes, *RSC Adv.*, **6(30)**, 25082–25093 **(2016)**

15. Moloudi K., Abrahamse H. and George B.P., Co-delivery of berberine and gold nanoparticles on liposomes for photodynamic therapy against 3D lung cancer cells, *Mater. Adv.*, **5(15)**, 6185–6195 **(2024)**

16. Narayanan M., Hussain F.A.J., Srinivasan B., Sambantham M.T., Al-Keridis L.A. and Al-Mekhlafi F.A., Green synthesis and characterization of copper-oxide nanoparticles by *Thespesia populnea* against skin-infection causing microbes, *J. King Saud Univ. Sci.*, **34(3)**, 101885 **(2022)**

17. Phull A.R., Ali A., Dhong K.R., Zia M., Mahajan P.G. and Park H.J., Synthesis, characterization, anticancer activity assessment and apoptosis signaling of fucoidan mediated copper oxide nanoparticles, *Arab. J. Chem.*, **14(8)**, 103250 **(2021)**

18. Qamar H., Rehman S., Chauhan D.K., Tiwari A.K. and Upmanyu V., Green synthesis, characterization and antimicrobial activity of copper oxide nanomaterial derived from *Momordica charantia*, *Int. J. Nanomed.*, **15**, 2541–2553 **(2020)**

19. Sathiyavimal S. et al, Green chemistry route of biosynthesized copper oxide nanoparticles using *Psidium guajava* leaf extract and their antibacterial activity and effective removal of industrial dyes, *J. Environ. Chem. Eng.*, **9(2)**, 105033 **(2021)**

20. Sen Srimoyee, Chatterjee Debasmita, Singh Banhishikha, Paira Krishnendu and Das Satadal, Direct effect of ultra diluted ethanolic extract of Apis mellifica on Escherichia coli and Staphylococcus aureus in Gallus gallus domesticus embryo model, *Res. J. Biotech.*, **19(6)**, 28-34 **(2024)**

21. Song D., Hao J. and Fan D., Biological properties and clinical applications of berberine, *Front. Med.*, **14(5)**, 564–578 **(2020)**

22. Sung H., Ferlay J., Siegel R.L., Laversanne M., Soerjomataram I., Jemal A. and Bray F., Global cancer statistics 2020: GLOBOCAN estimates of incidence and mortality worldwide for 36 cancers in 185 countries, *CA Cancer J. Clin.*, **71(3)**, 209–249 **(2021)**

23. Taebpour M., Arasteh F., Akhlaghi M., Haghirosadat B.F., Oroojalian F. and Tofighi D., Fabrication and characterization of PLGA polymeric nanoparticles containing berberine and its cytotoxicity on breast cancer cell (MCF-7), *Nanomed. Res. J.*, **6(4)**, 396–408 **(2021)**

24. Tavakoli S., Kharaziha M. and Ahmadi S., Green synthesis and morphology dependent antibacterial activity of copper oxide nanoparticles, *J. Nanostruct.*, **9(1)**, 163–171 **(2019)**

25. Upadhyay L.S.B., Tirkey A., Bhagat P., Singh S.K. and Mishra A., Green synthesis of copper oxide nanoparticles using *Solanum tuberosum* extract to mediate photocatalytic degradation of methylene blue, *Plasmonics*, **20**, 1–16 **(2025)**

26. Vanti G.L., Kurjogi M., Basavesha K.N., Teradal N.L., Masaphy S. and Nargund V.B., Synthesis and antibacterial activity of *Solanum torvum* mediated silver nanoparticle against *Xanthomonas axonopodis* pv. *punicae* and *Ralstonia solanacearum*, *J. Biotechnol.*, **309**, 20–28 **(2020)**

27. Wu C., Dong B., Huang L., Liu Y., Ye G., Li S. and Qi Y., SPTBN2, a new biomarker of lung adenocarcinoma, *Front. Oncol.*, **11**, 754290 **(2021)**.

(Received 20th August 2025, accepted 20th September 2025)